Biochimica et Biophysica Acta 1853 (2015) 1636–1645

Contents lists available at ScienceDirect

Biochimica et Biophysica Acta

journal homepage: www.elsevier.com/locate/bbamcr

N-linked Glycosylation of human SLC1A5 (ASCT2) transporter is critical for trafficking to membrane

Lara Console [a,b], Mariafrancesca Scalise [a], Zlatina Tarmakova [b], Imogen R. Coe [b], Cesare Indiveri [a,*]

[a] Department DiBEST (Biologia, Ecologia, Scienze della Terra) Unit of Biochemistry and Molecular Biotechnology, University of Calabria, Via P. Bucci 4C, 87036 Arcavacata di Rende, Italy
[b] Department of Chemistry and Biology, Ryerson University, 350 Victoria St., Toronto M5B 2K3, Canada

ARTICLE INFO

Article history:
Received 13 March 2015
Received in revised form 26 March 2015
Accepted 31 March 2015
Available online 7 April 2015

Keywords:
Glutamine
Plasma membrane
Transport
Liposomes
Protein stability

ABSTRACT

The human amino acid transporter SLC1A5 (ASCT2) contains two N-glycosylation sites (N163 and N212) located in the large extracellular loop. In the homology structural model of ASCT2 these Asn residues are extracellularly exposed. Mutants of the two Asn exhibited altered electrophoretic mobility. N163Q and N212Q displayed multiple bands with apparent molecular masses from 80 kDa to 50 kDa. N163/212Q displayed a single band of 50 kDa corresponding to the unglycosylated protein. The presence in membrane of WT and mutants was evaluated by protein biotinylation assay followed by immunoblotting. The double mutation significantly impaired the presence of the protein in membrane, without impairment in protein synthesis. [^{3}H]glutamine transport was measured in cells transiently transfected with the WT or mutants. N163/212Q exhibited a strongly reduced transport activity correlating with reduced surface expression. The same proteins extracted from cells and reconstituted in liposomes showed comparable transport activities demonstrating that the intrinsic transport function of the mutants was not affected. The rate of endocytosis of ASCT2 was assayed by a reversible biotinylation strategy. N212Q and N163/212Q showed strongly increased rates of endocytosis respect to WT. ASCT2 stability was determined using cycloheximide. N163Q or N163/212Q showed a slightly or significantly lower stability with respect to WT. To assess trafficking to the membrane, a brefeldin-based assay, which caused retention of proteins in ER, was performed. One hour after brefeldin removal WT protein was localized to the plasma membrane while the double mutant was localized in the cytosol. The results demonstrate that N-glycosylation is critical for trafficking.

1. Introduction

Amino acid flux through biological membranes and distribution to tissues are both finely controlled by numerous transporters belonging to different solute carrier (SLC) families. Many of these amino acid transporters are characterized functionally [1–5] but much is still unknown concerning their structure/function relationships, protein–protein interactions and trafficking. Among these transporters, SLC1A5, known as ASCT2, is one of the most attractive to study due to its involvement in cell signaling and relevance to human pathology. ASCT2 was proposed to be a sodium dependent antiporter accepting alanine, serine and cysteine as the major substrates and also glutamine, alanine, serine, asparagine, threonine, valine and methionine [6,7]. More recent studies performed in proteoliposomes on the rat or human proteins revealed that ASCT2 is functionally asymmetrical since the substrate alanine, valine and methionine can be only inwardly transported [8,9]. The ability of ASCT2 to transport glutamine, along with its ubiquitous tissue expression, suggests that this transporter is a key player in glutamine homeostasis [10,11]. The potentially important role of ASCT2 in human cancer emerged from the finding that it is over-expressed in several malignancies together with SLC7A5, also known as LAT1 [1,12,13]. Over-expression of ASCT2 and LAT1 increases glutamine uptake allowing cancer cells to produce metabolic energy from glutamine by a modified biochemical pathway, typical of cancer cells, involving glutaminase and some enzymes of the citric acid cycle [14,15]. ASCT2 has been proposed, in association with LAT1, to be a plasma membrane component of the mTOR signaling pathway [16,17]. Therefore, ASCT2 represents a potential pharmacological target in cancer as well as in pathologies linked to derangements of the mTOR pathway, such as obesity, type 2 diabetes and neurodegeneration [18]. Over the years, several studies have attempted to identify potent and

Abbreviations: $C_{12}E_8$, octaethylene glycol monododecyl ether; BFA, brefeldin-A; DMEM, Dulbecco's Modified Eagle Medium; FBS, fetal bovine serum; TX-100, Triton X-100; NP-40, nonidet; MeAIB, α-(methylamino)isobutyric acid; BCH, 2-aminobicyclo-(2,2,1)-heptane-2-carboxylic acid; ER, Endoplasmic reticulum; MESNA, 2-mercaptoethanesulfonic acid

* Corresponding author at: Department DiBEST(Biologia, Ecologia e Scienze della Terra) University of Calabria Via P. Bucci cubo 4C, 87036 Arcavacata di Rende (CS) Italy. Tel.: +39 0984 492939; fax: +39 0984 492911.

http://dx.doi.org/10.1016/j.bbamcr.2015.03.017
0167-4889/

specific inhibitors of ASCT2 by combining bioinformatics and experimental strategies [19–21]. However, the main challenge in performing large scale screening of pharmacological compounds that interact with ASCT2 is the lack of three-dimensional structure of the transporter. A crystallographically derived structure of plasma membrane transporters of high eukaryotes is not available, with the exception GLUT1, which was solved using an inactive form of the protein [22]. Therefore, data on structure/function relationships for ASCT2 are derived from homology structural models built using, as template, the glutamate transporter Glt_{ph} from *Pyrococcus horikoshii*, which possesses enough similarity to human and rat ASCT2 [23]. From these studies it was deduced that the rat orthologue, consisting of 16 cysteine (Cys) residues in its primary structure, harbors the typical metal binding motif, CXXC, which shows high reactivity towards mercury compounds [24]. The human orthologue contains only 8 Cys residues and lacks of the CXXC motif. Even though the overall sequence identity between the rat and human orthologues is more than 79%, local alignment shows a stretch of 31 amino acids (aa 200–229), where identity is lower than 14%, suggesting that the human and rat orthologues have different properties and, hence, the rat protein cannot be used as a model for the human transporter. The presence of several Cys residues, however, does allow the human orthologue to interact with SH reagents and this completely abolishes transport activity. These data indicate that the Cys residues are important for transport and are accessible to SH reagents [25]. There is considerably less information on the regulation of transport activity and cell expression of ASCT2 compared to structural features [1]. Very recently it was shown that transport reaction is modulated by membrane potential and that the sodium coupled glutamine/amino acid antiport is electrogenic. Moreover, internal sodium also regulates transport by allosteric effects. Furthermore, it has been demonstrated that ASCT2 interacts with the scaffold protein PDZK1 [25] suggesting that protein–protein interactions may be involved in regulation of the transporter. Some information is available on ASCT2 promoter and regulation via a Raf-MEK-ERK kinase cascade [26]. A completely unexplored aspect of regulation of ASCT2 and most amino acid transporters is the trafficking to plasma membrane. N-glycosylation has been linked to trafficking of transporters [27–29] and represents the most frequent post translational modification of human proteins since more than 50% of proteins are glycosylated [30,31]. We hypothesized that glycosylation could play a role in the trafficking of ASCT2 in mammalian cells and role of glycosyl moieties of the protein in the process of delivery to plasma membrane was assessed. Two putative glycosylation sites were predicted by bioinformatics and were subject to site-directed mutagenesis. The effects on function and targeting of both WT and mutant isoforms of ASCT2 are reported here and represent, to our knowledge, the first evidence on the role of glycosyl moiety in trafficking for a human amino acid transporter.

2. Materials and methods

2.1. Materials

Human embryonic kidney HEK293 cells were obtained from the American Type Culture Collection (ATCC). Tissue culture media, fetal bovine serum, Alexa Fluor 594 anti rabbit and transfection reagent Lipofectamine were obtained from Life Technologies. PNGase F, restriction endonucleases and other cloning reagents from NEB (New England Biolabs); sulfo-NHS-SS-biotin from Thermo Scientific; ECL plus, Hybond ECL membranes from GE Healthcare; L-[^{3}H] glutamine from Perkin Elmer; the anti rabbit IgG HRP conjugate from Cell Signaling; the QIAEX II Gel Extraction Kit from Qiagen; the Polyjet transfection reagent was from SignaGen Laboratories; the protease inhibitor mix from Roche; the rabbit anti-ASCT2 from Millipore, the plasmid p3XFLAG-CMV-7.1, $C_{12}E_8$, Amberlite XAD-4, egg yolk phospholipids (3-sn-phosphatidylcoline from egg yolk), Sephadex G-75, L-glutamine, cycloheximide, rabbit anti-FLAG, MESNA, streptavidin beads and all the other reagents were from Sigma-Aldrich.

2.2. Site-directed mutagenesis

The cDNA of ASCT2 was subcloned into p3XFLAG-CMV-7. p3XFLAG-CMV-7.1 is a 4717bp expression vector used to establish transient expression of N-terminal FLAG fusion protein in mammalian cell. The vector encodes three-FLAG epitope (DYKDHDGDYKDHDIDYKDDDDK) at the N-terminus inserted after Met. The plasmid is a shuttle vector for *Escherichia coli* with ampicillin resistance and contains a CMV promoter. This construct was used to introduce the mutations in the ASCT2 protein. The amino acid replacements were performed with complementary mutagenic primers (N163Q forward CTCCGCCGCCAT CCAAGCCTCCGTG, N163Q reverse CACGGAGGCTTGGATGGCGGCGGAG, N212Q forward TATGAAGAGAGGCAAATCACCGGAACC, N212Q reverse GGTTCCGGTGATTTGCCTCTCTTCATA) using the overlap extension method and the High-Fidelity PCR System [32,33]. The PCR products were purified by the QIAEX II Gel Extraction Kit (QIAGEN), digested with HindIII and KpnI (restriction sites added at the 5′ end of forward and reverse primers, respectively) and ligated into the same mammalian expression vector. All mutations were verified by DNA sequencing.

2.3. Cell culture

HEK293 cells were maintained in Dulbecco's Modified Eagle Medium (DMEM) supplemented with 10% (v/v) fetal bovine serum (FBS), 1 mM glutamine and 1 mM sodium pyruvate. Cells were grown on 10 cm^2 plates at 37 °C in a humidified incubator and a 5% CO_2 atmosphere.

2.4. SDS-polyacrylamide gel electrophoresis and western blotting

The human cells or rat kidney cortex (where ASCT2 is expressed [9]) homogenate was solubilized in RIPA buffer (20 mM Tris–HCl pH 7.5, 150 mM NaCl, 1 mM EDTA, 1 mM EGTA, 1% NP-40, 1% sodium deoxycholate) supplemented with protease inhibitors. The proteins were separated on a 12% polyacrylamide gel and transferred to nitrocellulose membrane. The nitrocellulose membrane was treated with blocking buffer for 1 h at room temperature. The membrane was then incubated in a solution of the primary antibody, a rabbit anti-FLAG or a rabbit anti-ASCT2 and diluted 1:5000 or 1:2000 with the blocking buffer overnight at 4 °C, respectively. The blot was washed three times at room temperature. It was then incubated with the secondary antibody, anti-rabbit IgG, a peroxidase-linked species-specific whole antibody diluted 1:10,000 with the blocking buffer for 1 h at room temperature and revealed by chemiluminescence.

2.5. Transport measurements in cells

HEK 293 cells were seeded onto 12 well plates and cultured using standard culturing conditions until they reached 80% confluence. Cells were transfected with Lipofectamine transfection reagent according to the manufacturer's procedures: 0.5 μg of p3XFLAG-CMV-7.1-ASCT2 WT, p3XFLAG-CMV-7.1-N161Q, p3XFLAG-CMV-7.1-N212Q and p3XFLAG-CMV-7.1-N163/212Q diluted in 50 μL Opti-MEM were combined with 1.5 μl of Lipofectamine in 50 μL Opti-MEM. After 20 min incubation at room temperature the mixture was added to cell culture for 5 h at 37 °C in a CO_2 incubator. After incubation the medium was replaced with DMEM supplemented with 10% (v/v) FBS, 1 mM Gln and 1 mM sodium pyruvate; 24 h after transfection, cells were used for transport assay of L-[^{3}H]glutamine. Cells were rinsed twice with warm transport buffer: 20 mM THCl pH 7.4, 3 mM K_2HPO_4, 1 mM $CaCl_2$, 5 mM glucose, 130 mM NaCl, 10 mM BCH, and 10 mM MeAIB. Radiolabeled 10 μM [^{3}H]glutamine was added and the transport reaction was terminated at the indicated times by discarding the uptake

buffer and rinsing the cells three times with the same ice-cold transport buffer (0.5 ml per well per rinse) plus 10 μM Mersalyl. Cells from each well were solubilized in 500 μl of 1% TX-100 solution. Cell extracts were counted for radioactivity (400 μl). The remaining 100 μl in each well were used for protein concentration assay. Na^+-dependent glutamine transport was evaluated by subtracting the transport values of each ASCT2 mutant from those deriving from cells transfected with empty vector.

2.6. Transport measurements in proteoliposomes

HEK 293 cells were transiently transfected as above described then lysed with RIPA Buffer. Total lysate (20 μg) was reconstituted in proteoliposomes using a batch wise procedure [34]. The mixed micelles containing detergent, protein and phospholipids were incubated with 0.5 g Amberlite XAD-4 resin under rotatory stirring (1200 rev/min) at room temperature (25 °C) for 40 min [35]. The composition of the initial mixture used for reconstitution was: 20 μg protein, 120 μL of 10% (v/v) $C_{12}E_8$, 100 μL (v/v) of 10% egg yolk phospholipids (w/v) in the form of sonicated liposomes, 10 mM L-glutamine and 20 mM Tris/HCl pH 7.0 in a final volume of 700 μL [25]. Transport was started by adding 50 μM [^{3}H]glutamine to 100 μL of proteoliposomes previously subjected to Sephadex G75 chromatography to remove external substrate. Transport was stopped at the indicated times according to stop inhibitor method and radioactivity was counted as previously described [25]. To calculate kinetic parameters, transport rates were measured at 10 min transport (i.e., within the initial linear range of the time course in proteoliposomes) as dependence on [^{3}H]glutamine concentration ranging from 10 μM to 300 μM. Experimental data were fitted in Michaelis–Menten equation using non-linear fitting analysis by Grafit software (version 5.0.13).

2.7. In vitro endoglycosidase treatment

Cells expressing WT and mutant ASCT2 were solubilized as above. N-glycosidase F was added to 20 μg of total lysate for 1 h at 37 °C following manufacturer's procedures. The reaction was then terminated by storage at −80 °C. Frozen aliquots were thawed and subjected to SDS-PAGE followed by immunoblotting analysis.

2.8. Confocal microscopy

HEK 293 cells were seeded onto cover slip and cultured using standard culturing conditions until 50–70% confluence. Cells were transfected with PolyJet transfection reagent according to the manufacturer's procedures: 0.5 μg of p3XFLAG-CMV-7.1-ASCT2 WT, p3XFLAG-CMV-7.1-N161Q, p3XFLAG-CMV-7.1-N212Q and p3XFLAG-CMV-7.1-N163/212Q diluted in 25 μl of serum-free DMEM was combined with 1.5 μl of PolyJet diluted in the same medium. After 15 min incubation at room temperature the mixture was added to the cell culture; 24 h after transfection cells were fixed with 4% (w/v) paraformaldehyde (15 min; 37 °C). After rinsing with PBS, cells were blocked with 10% (v/v) bovine serum albumin in PBS for 45 min at room temperature. Cells were then incubated with the rabbit monoclonal anti-FLAG antibody at 1:500 dilution for 1 h followed by Alexa Fluor 594-conjugated anti-rabbit secondary antibody at 1:300 dilution for 45 min. The cover slips were then washed three times in PBS and mounted with DAKO mounting medium. Confocal microscopy was performed using a Leica confocal microscope (40× oil immersion lens). To evaluate ER to Golgi trafficking, transfected cells were incubated with 5 μM Brefeldin-A for 7 h to inhibit ER to Golgi protein trafficking and then rinsed twice with 1× PBS to washout BFA. After that, cells were incubated in FBS free DMEM containing cycloheximide (1 mM) for increasing time points.

2.9. Assessment of ASCT2 endocytosis by reversible biotinylation

HEK293 cells seeded on poly-D-lysine-coated 6-well plates and cultured using standard culturing conditions up to 70–80% confluence. Cells were transfected with PolyJet transfection reagent according to the manufacturer's procedures with 1 μg of p3XFLAG-CMV-7.1-ASCT2 WT, p3XFLAG-CMV-7.1-N161Q, p3XFLAG-CMV-7.1-N212Q and p3XFLAG-CMV-7.1-N163/212Q. On the day of the endocytosis assay, the cells were washed twice in ice-cold PBS (pH 8.0) and incubated with 0.75 ml of disulfide-cleavable biotin (sulfo-NHS-SS-biotin) diluted in PBS (pH 8.0) for 45 min at 4 °C. Sulfo-NHS-SS-biotin does not permeate plasma membrane, thus, only cell surface proteins are covalently labeled on extracellular Lys. Then, cells were incubated for 30 min in PBS containing 100 mM glycine to quench all non-reacting biotin. Cells were incubated again in pre-warmed DMEM containing 10% (v/v) FBS at 37 °C and 5% CO_2 for increasing times (0–60 min) to allow the endocytosis of labeled surface protein. At the end of each time point, cells were immediately rinsed with PBS and incubated with the cell-impermeant reducing agent 100 mM 2-mercaptoethanesulfonic acid (MESNA) solubilized in PBS, pH 8.0 at 4 °C for 40 min and washed twice in ice-cold PBS containing 120 mM iodoacetamide. MESNA was used to cleave the NHS-SS-biotin disulfide bond and to strip off any residual surface biotin. The endocytated biotinylated proteins protected from the stripping were the only biotinylated protein. Cells were then solubilized in RIPA buffer, and biotinylated ASCT2 was isolated using monomeric streptoavidin beads. Using this procedure the endocytated ASCT2-NHS-SS-biotin which was protected from reduction, could be subsequently isolated by streptavidin affinity chromatography and detected by immunoblotting. To determine the endocytic rate, the amount of internalized ASCT2 was compared to the total surface control labeled at time zero. The MESNA stripping efficiency was greater than 95% based on reduction of the disulphides ASCT2-NHS-SS-biotin. After immunoblotting, the intensity of the band derived from cells immediately exposed to MESNA was subtracted as background from all other band intensities [27].

2.10. Evaluation of protein stability

HEK293 cells were seeded on 6-well plates and cultured using standard culturing conditions up to 70–80% confluence. Cells were transfected with PolyJet transfection reagent according to the manufacturer's procedures with 1 μg of p3XFLAG-CMV-7.1-ASCT2 WT, p3XFLAG-CMV-7.1-N163Q, p3XFLAG-CMV-7.1-N212Q and p3XFLAG-CMV-7.1-N163/212Q. Cells were incubated over increasing times with cycloheximide (20 μg/ml) to inhibit further protein synthesis. At each time point cells were harvested, lysed, and subjected to SDS-PAGE followed by immunoblot analysis [36,37].

2.11. Other methods

The homology structural model of hASCT2 was built using the crystal structure (1XFH) of the glutamate transporter homologue from *P. horikoshii* as a template. The optimized alignment was used to run the program Modeller 9.11. The N-glycosylation sites were predicted by NetNGlyc 1.0 Server. The amount of protein in total lysate was calculated with Lowry-Folin assay. The quantification of protein bands detected by immunoblotting was estimated by using the Chemidoc imaging system equipped with Quantity One software (Bio-Rad) as previously described [38].

3. Results

3.1. Bioinformatic and structural analysis

Bioinformatic analysis using NetNGlyc 1.0 revealed that ASCT2 contains two putative N-glycosylation sites, corresponding to residues

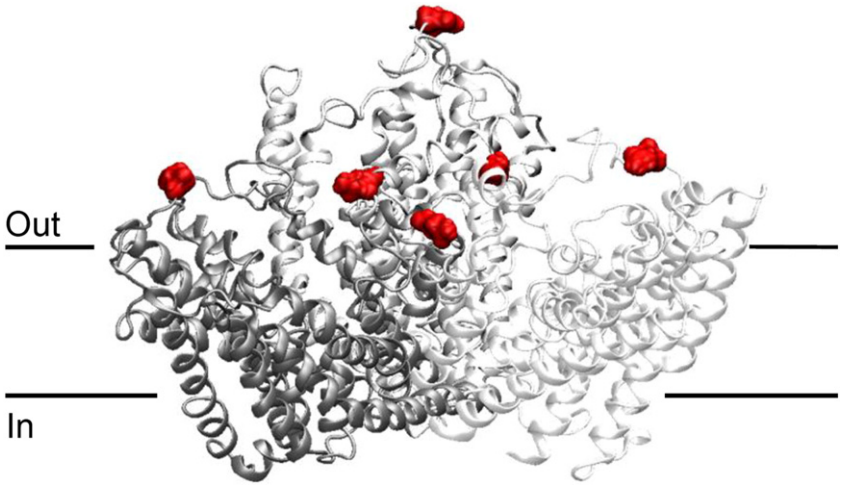

Fig. 1. Homology model of hASCT2. Overall structure of trimeric hASCT2 viewed parallel to membrane. Monomers are distinguished by different gray scales. The two N-glycosylated residues (N163 and N212) are represented in a space-filled view and highlighted. The membrane is indicated by black lines.

N163 and N212 which are located in the large extracellular loop between the third and fourth transmembrane segment. It was previously demonstrated that functional ASCT2 has an oligomeric structure consisting of two or three subunits similar to the glutamate transporter of *P. horikoshii* [23]. In this oligomeric form, all six putative glycosylated Asn residues protrude towards the extracellular environment (Fig. 1). This arrangement agrees with the finding that the protein is structurally and functionally asymmetric and all the subunits show the same orientation in the reconstituted system as in the native membrane [8,25].

3.2. Identification of N-linked glycosylation sites

We hypothesized that the glycosyl moieties linked to the Asn residues might be involved in cell-surface expression of the transporter. To confirm that these residues were indeed glycosylated, we performed single or double substitution of the two Asn residues (N163 and N212) of the consensus sequence for N-glycosylation (N-X-S/T), with glutamine by site-directed mutagenesis and tested for loss of glycosylation. HEK293 cells were transiently transfected with a plasmid encoding the full-length WT or mutant ASCT2 tagged at the N-terminus with FLAG. The effect of removal of the putative N-glycosylation sites and treatment with N-glycanase on the molecular weight of ASCT2 were first evaluated. In the absence of glycosidase treatment, immunoblotting with anti-FLAG antibody highlighted that HEK293 cells, transfected with WT ASCT2, displayed several bands with apparent molecular mass varying from about 80 kDa to 50 kDa (Fig. 2). Cells transfected with the single mutant N163Q or N212Q displayed bands from about 70 kDa to 50 kDa, respectively. The double mutant N163/212Q displayed a single band of about 50 kDa, confirming that indeed the two glycosylation sites carry glycosyl moieties which are completely absent in the double mutant. After treatment of WT and single mutants with N-glycanase, the protein patterns were converted to that of the double mutant, i.e., a single protein band of about 50 kDa was present (Fig. 2A). Note that the apparent molecular mass of N-glycanase treated protein corresponded to that of the ASCT2 over-expressed in *P. pastoris*, i.e., without glycosyl moieties [8]. These data confirm that the WT protein contains glycosyl moieties linked to the N-glycosylation sites at residues N163 and N212. The same experiment was performed on protein extracted from rat kidney; also in this case, ASCT2 shows glycosylation moieties, similar to those of protein over-expressed in HEK293 cells, which disappeared upon N-glycanase treatment (Fig. 2B).

3.3. Membrane biotinylation and transport assay

We anticipated that N-glycosylation would influence the presence of ASCT2 at the plasma membrane. To confirm this, the relative presence of ASCT2 (WT and mutants) was evaluated using a protein biotinylation assay involving membrane-impermeant sulfo-NHS-biotin. Biotinylated proteins were collected with streptavidin resin, subjected to SDS-PAGE followed by immunoblotting with anti-FLAG antibody. Interestingly, the presence at the surface of the double mutant was significantly reduced in comparison to WT, while the single mutants showed a comparable or slightly lower level to WT (Fig. 3A). This difference is not due to decreased overall protein being produced because total

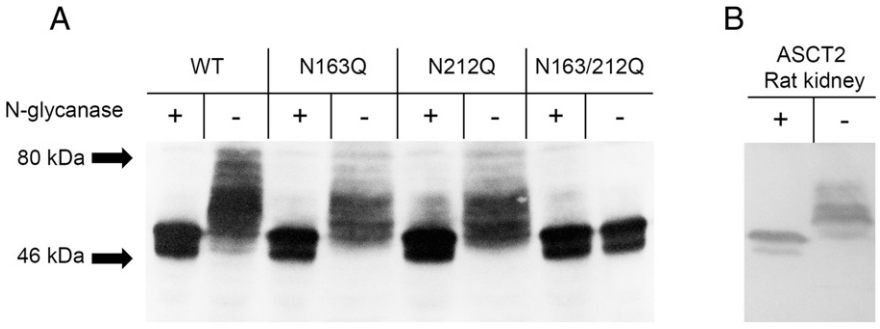

Fig. 2. Effect of N-glycosidase F on ASCT2. (A) Whole extracts of HEK293 cells transiently transfected with ASCT2 WT or mutant constructs were separated by 12% SDS-polyacrylamide gel electrophoresis (20 μg protein/lane), blotted, and probed with anti-FLAG antibody as described in Materials and Methods. Lanes marked with plus were treated *in vitro* with N-glycosidase F (500 u) for 1 h at 37 °C. (B) Whole extract of rat kidney brush border vesicles were separated by 12% SDS-polyacrylamide gel electrophoresis (80 μg protein/lane), blotted, and probed with anti-ASCT2 antibody as described in Materials and Methods. Lanes marked with plus were treated *in vitro* with N-glycosidase F (500 u) for 1 h at 37 °C.

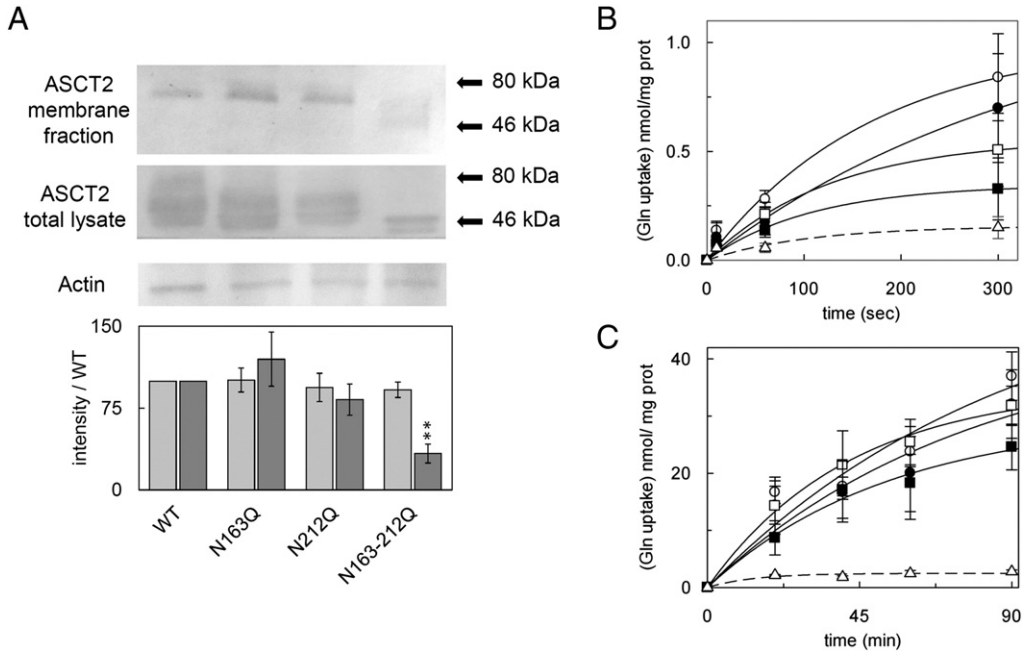

Fig. 3. Role of glycosylation on presence of ASCT2 at the plasma membrane and on functionality. A) Cell surface biotinylation of ASCT2 in HEK293 cells. Surface protein fractions obtained by incubation of total lysates with avidin beads, was entirely loaded on SDS-PAGE for western blot analysis (ASCT2 membrane fraction); ASCT2 total lysate is shown as control; actin is shown as an additional control of total lysate loading. ASCT2 or actin was immunodetected by anti-FLAG or anti-actin, respectively. Representative blots are shown. The histogram represents scanning densitometry of 3 immunoblots with similar results for quantification; light gray columns represent the percentage of band intensity compared to WT of total protein extract; dark gray columns represent the percentage of band intensity compared to WT of surface protein fractions. Significantly different from WT as estimated by Student's t-test (**$P < 0.01$). B) Intact HEK293 cells transiently transfected with empty vector (Δ dashed line), WT (○), N163Q (●), N212Q (□) or N163/212Q (■) constructs were tested for uptake of [^{3}H] glutamine. Transport reaction was terminated at the indicated times as described in Materials and methods. C) Lysate from HEK293 cells transiently transfected with empty vector (Δ dashed line), WT (○) N163Q (●) N212Q (□) or N163/212Q (■) constructs were reconstituted in proteoliposomes and tested for uptake of [^{3}H]glutamine. The transport reaction was stopped at the indicated times as described in Materials and methods. Results are means ± S.D. from three independent experiments.

protein levels and transfection levels were equivalent for all constructs (Fig. 3A).

ASCT2 transport of [^{3}H] glutamine was measured in cells following transient transfection with the WT or glycosylation-deficient mutants (N163Q, N212Q and N163/212Q) in comparison to empty vector. The single mutant, N212Q, and double mutant, N163/212Q, exhibited transport activities of about half and one fourth, respectively, of WT levels (Fig. 3B) which correlates with a lower expression of these mutants at cell-surface (Fig. 3A, membrane fraction). In contrast, the single mutant N163Q, exhibited a transport activity that was comparable to WT. To determine if mutations affect intrinsic transport activity, equal amounts of protein extracted from HEK293 cells, transfected with WT, mutant or empty vector constructs, were reconstituted in liposomes. Transport activity was measured as uptake of [^{3}H] glutamine in exchange with unlabeled glutamine in all the samples in comparison to extract from cell transfected with empty vector (Fig. 3C). The feature of this technique allowed us to abolish the differences in transport activity deriving from different expression in plasma membrane among the four constructs. These analyses highlighted that all mutants possess transport activity comparable to WT indicating that absence of glycosylation does not affect the intrinsic activity of ASCT2 but only the amount of protein reaching cell surface (Fig. 3C). In the same proteoliposomes model, Km values for WT, N163Q, N212Q and N163/212Q were measured as described in Materials and methods being 31.4 ± 4.7 μM, 35.6 ± 8.3 μM, 29.3 ± 5.4 μM and 38.3 ± 6.3 μM, respectively. Km values for mutants are not significantly different from WT as determined from ANOVA one way test for $p < 0.05$.

3.4. Endocytosis of surface ASCT2

Changes in the rate of endocytosis could be responsible for altering the surface expression and function of ASCT2. Using a reversible biotinylation strategy, the endocytosis of ASCT2 was examined by quantifying the fraction of surface protein that moves in a time-dependent manner (from 15 to 60 min) into the cytosol. Data show that single (N212Q) and double (N163-212Q) glycosylation mutants have increased rates of endocytosis compared to WT (Fig. 4). WT protein can be visualized (by immunoblotting) intracellularly at 60 min (Fig. 4A), while single (N212Q) and double (N1630212Q) are internalized much sooner (by 30 min). The percentage of ASCT2 internalization was enhanced in N-linked glycosylation double mutants over the same time interval (Fig. 4B). Interestingly, N163Q showed an internalization pattern similar to WT, while the mutant N212Q behaved similarly to the double mutant. The initial rate of ASCT2 internalization was estimated by fitting the fraction of internalized ASCT2 as a function of time (Fig. 4A and B). As shown in Table 1, the single mutant N212Q and the double N163/212Q showed significantly enhanced internalization rate respect to the WT. These data confirm the earlier findings (Fig. 3) which suggest that the glycosylation deficient mutants N212Q and N163-212Q are present at the membrane at lower levels than WT.

3.5. Analysis of stability of ASCT2

To determine the importance of N-glycosylation on ASCT2 stability, HEK293 cells were transiently transfected with ASCT2 WT or mutants and incubated with cycloheximide (20 μg/ml) to inhibit protein synthesis (Fig. 5). After incubation for 2, 4 and 10 h, cells were harvested, lysed, and subjected to SDS-PAGE and immunoblot analysis (Fig. 5). Band density was quantified and normalized so that the density at time 0 was 100%. Data show (Fig. 5A and C) that WT and N212Q are approximately equivalently stable up to 10 h. Mutant N163Q possessed stability slightly lower than WT (Fig. 5B). However, in contrast, the N163/212Q double mutant showed a clear decrease in stability after 10 h incubation (Fig. 5D). To confirm these data, same cells were analyzed by

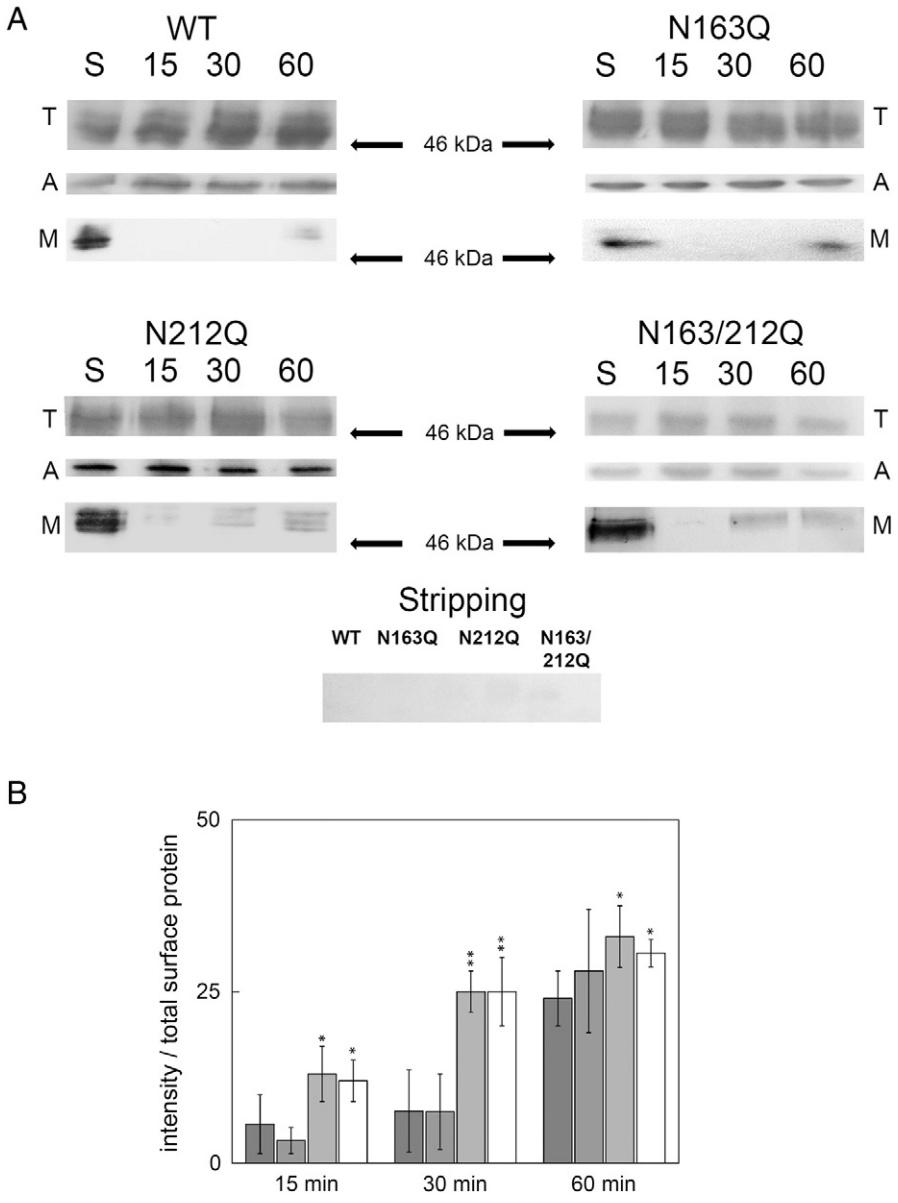

Fig. 4. Time course for endocytosis of surface hASCT2. HEK293 cells expressing ASCT2 WT or mutant constructs were surface-biotinylated with cleavable biotin, incubated for different times at 37°C and stripped with cell-impermeant MESNA. Biotinylated proteins were isolated using avidin and quantified by immunoblot analysis as described in Materials and methods. A) Representative immunoblots for total surface (S) and for the internalized hASCT2 at different times (15, 30 and 60 min) are shown. Stripping efficiency confirmed approximately 95% removal of NHS-SS-biotin from cell surface protein. T indicates the ASCT2 total lysate shown as control; A indicated actin, shown as loading control for ASCT2 total lysate; M indicates the ASCT2 membrane fraction obtained as described in legend of Fig. 3 and Materials and methods. ASCT2 or actin has been immunodetected by anti-FLAG or anti-actin, respectively. B) Quantification of internalized hASCT2. Data are derived from the band intensity at the different time points (15, 30, 60 min) as % comparison of the total surface protein (S). Dark gray represents WT, gray represents N163Q, light gray represents N212Q and white represents N163/212Q. Results are means ± S.D. from three independent experiments. Statistical analysis was performed for each mutant respect to the corresponding WT by Student's t-test, at the different times. Significantly different (*P < 0.05; **P < 0.01).

confocal microscopy after treatment with cycloheximide for varying times. Confocal analysis confirmed the previous data that such cells transfected with single mutants N163Q and N212Q displayed a loss of signal from the plasma membrane similar to that of WT at 7 h (Fig. 5E) while the double mutant showed strikingly less signal at the plasma membrane for all time points. By 7 h, fluorescent signal had nearly disappeared, indicating that the double mutant was less stable than either WT or single mutants and confirming western blot analysis (Fig. 5A–D). These results established that WT and single mutants were more stable in the membrane with respect to the N163/212Q double mutant.

Table 1
Effect of N-linked glycosylation on the initial rate of endocytosis and the half-life time of ASCT2 in HEK-293 cells. Data were obtained as described in Figs. 4 and 5. The initial rate of internalization was calculated by fitting the fraction of internalized ASCT2 as a function of time. The Log of the percentage of density (Fig. 5) was plotted versus time and half-life was calculated from the Log of 50%.

	WT	N163Q	N212Q	N163-212Q
Initial rate of internalization	0.4	0.5	1.2	1.2
Half-life time (h)	79	40	29	12

3.6. Trafficking of ASCT2 from the ER to the plasma membrane

The different levels of transporter at the cell-surface may result from variations of endocytosis, degradation and/or altered trafficking from ER to plasma membrane as a consequence of the lack of N-glycosylation

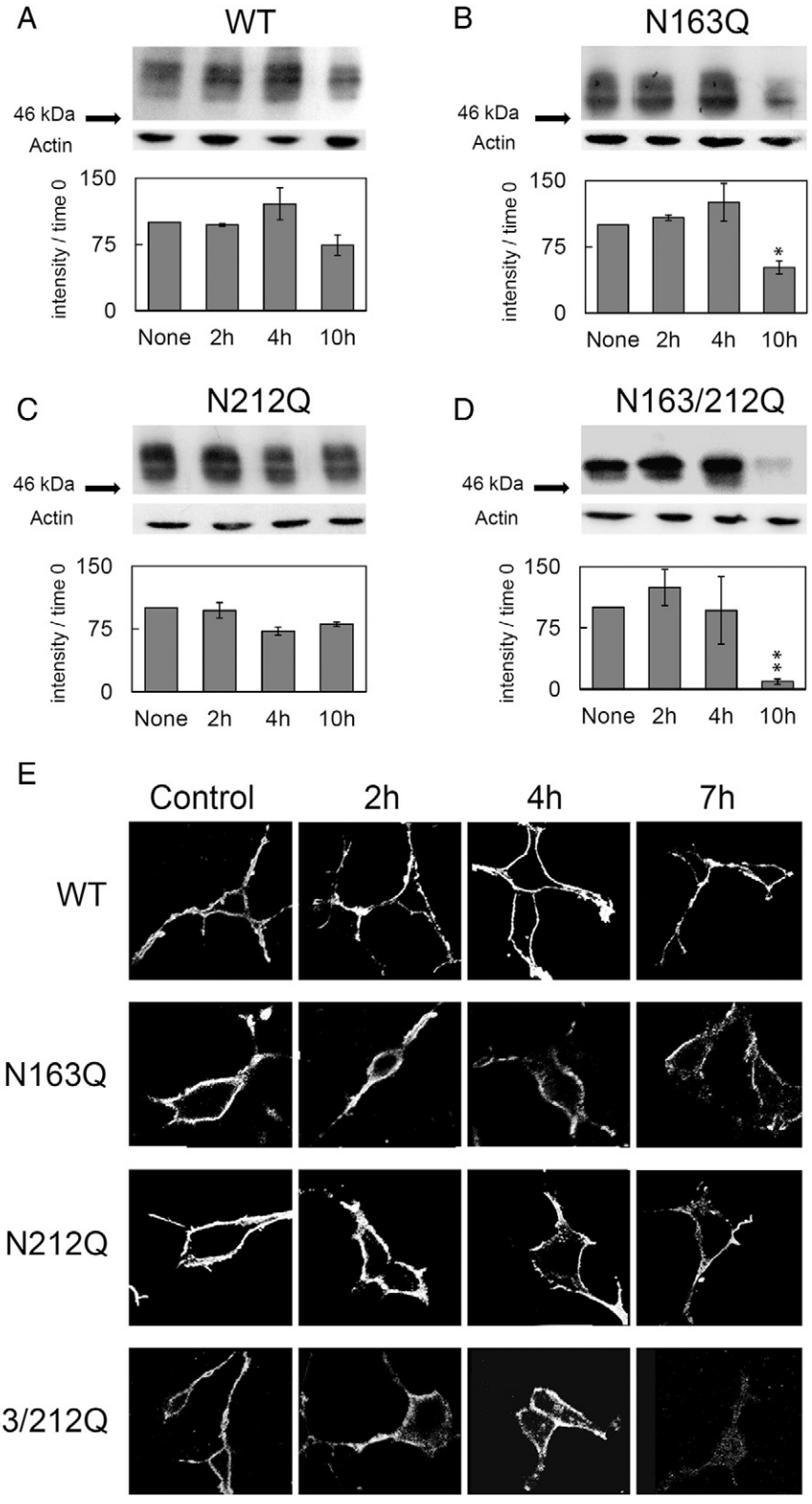

Fig. 5. Stability of ASCT2 varies with glycosylation level. HEK293 cells were transiently transfected with ASCT2 WT (A) or N163Q (B), N212Q (C), N163/212Q (D). After 24 h, cells were cultured in the presence of cycloheximide (20 μg/ml) and lysed at 0, 2, 4, and 10 h. Cell lysates were separated by SDS-PAGE and subjected to immunoblot analysis using anti FLAG-antibody as described in Materials and methods. Anti actin is used as loading control. The band intensity, measured and normalized so that the density at time 0 was 100%, was plotted. Significantly different from WT as estimated by Student's t-test (*$P < 0.05$; **$P < 0.01$). Representative immunoblots are shown. Results are means ± S.D. from three independent experiments. (E) The same samples from A–D were subjected to confocal analysis. Cells were transiently transfected with ASCT2 WT or mutant constructs. After 24 h, cells were cultured in the presence of cycloheximide (20 ug/ml), fixed at 0, 2, 4, 7 h and analyzed by confocal microscopy as described in Materials and methods. Confocal images show a single, representative, section of a Z-series taken through the entire cell.

[31]. To assess the contribution of trafficking to the presence of ASCT2 at the membrane, we repeated previous assays in the presence of brefeldin (BFA), an inhibitor of trafficking between the ER and plasma membrane [39]. Treatment with BFA led to retention of tagged-ASCT2 (whether mutant or WT) inside the cell i.e. in the ER (Fig. 6). Removal of BFA was followed by monitoring of ASCT2 trafficking over the course of

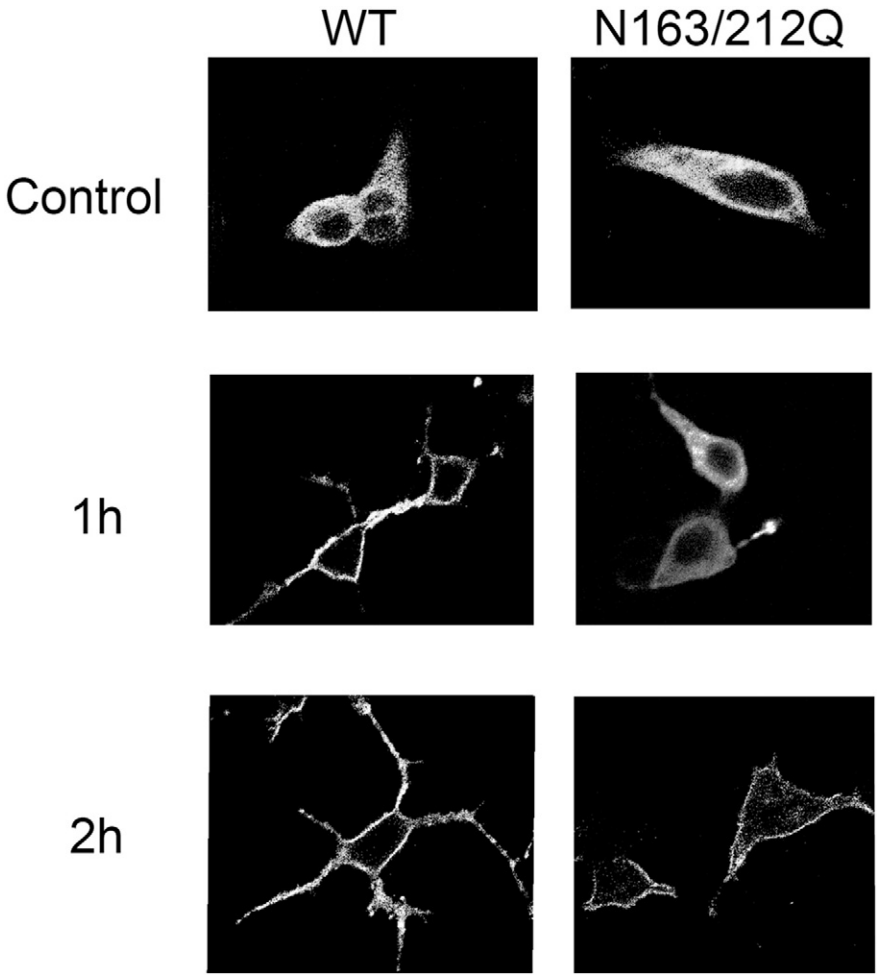

Fig. 6. Trafficking of ASCT2 from the ER to the plasma membrane varies with level of glycosylation. HEK293 cells transiently transfected with ASCT2 WT or N163/212Q constructs were treated with BFA (5 μM, 7 h). hASCT2 was retained in the ER and then rescued by BFA washout. Cells were fixed and labeled at the indicated times as described in Materials and methods. Confocal images show a single, representative, section of a Z-series taken through the entire cell.

the next 2 h and confocal microscopy analyses revealed that WT protein could be seen in the plasma membrane after the first hour. On the contrary, double mutant was located in the cytosol and only after two hours some signal was associated with the plasma membrane. This delay in reaching plasma membrane supports our hypothesis that absence of glycosylation at N163 and N212 results in a delayed trafficking of newly synthesized protein to the plasma membrane.

4. Discussion

One of the major, but still unsolved, fundamental biology issues concerning ASCT2 has been clarified in the study presented here. Using different experimental approaches, we have confirmed that transiently transfected ASCT2 is trafficked to plasma membrane within 1 h and then is internalized to be degraded. We show here that the overall process requires the presence of N-glycosyl moieties on residues N163 and N212. The homology structure of ASCT2 built on the basis of the bacterial Glt_{ph} structure [23], highlights that the two predicted N-glycosylation sites and hence, the associated glycosyl moieties are exposed towards the external environment, as expected. Functional data, derived from previous studies, show that the orientation of ASCT2 is as depicted in Fig. 1, both in native and in artificial membranes [8,25]. We demonstrated the involvement of the glycosyl moieties in delivery of ASCT2 to plasma membrane and demonstrated that at least one of the glycosyl moieties of ASCT2 is required for effective protein targeting to the plasma membrane. Abrogation of both glycosylation sites led to the most striking effects but interestingly glycosylation on the N212 site appears to be more critical to presence of the protein at the plasma membrane than that on N163, since the surface expression of the N212Q mutant is more similar to the double mutant than N163. Importantly, functional assays of the glycosylation-deficient ASCT2 constructs in native cell membranes and in proteoliposomes, demonstrated that presence or absence of N-glycosylation moieties has no influence on the intrinsic function of the transporter. Indeed, all three mutants are fully functional when assayed in proteoliposomes. This experimental strategy allows measurement of transport activity of solubilized total expressed protein, even if not targeted to the plasma membrane. In contrast, transport assays in intact cells detect only the plasma membrane targeted protein. Kinetic analyses revealed very similar Km for WT and mutants indicating that all the proteins are properly folded. These findings are in line with previous data on the endogenous protein, extracted in native form from HeLa cells and reconstituted in proteoliposomes before and after glycosidase treatment [25] confirming that glycosylation does not play a role in functionality once the transporter is in place. Similar roles of glycosylation were described for other transporters [40] such as the intestinal anion exchanger (SLC26A3) and the carnitine transporter (OCTN2, SLC22A5). Indeed, the functional properties of the deglycosylated anion exchanger were not appreciably modified, while its membrane expression was significantly decreased [29]. In the case of OCTN2, it was suggested that glycosylation has a role in trafficking even though it could not be excluded a minor role in substrate binding [41]. In other cases, such as

the GLUT1 or the dopamine transporter (DAT), N-glycosylation plays roles both in trafficking and in transport function [27,42,43].

In the case of ASCT2, the presence of several species with different apparent molecular mass in the total cell lysate (Fig. 2) compared to a single protein band in the plasma membrane fraction (Figs. 3 and 4) suggests that the plasma membrane-associated isoform is homogeneously glycosylated. The other observed species represents, thus, different stages of glycosylation or progressive degradation of the internalized protein. These data correspond with previous findings for other proteins which suggest that N-glycosylation is associated with protein stability [30] and that absence of glycosyl moieties resulted in a faster degradation. Indeed, confocal images (Fig. 5E) showed intracellular fluorescence associated with the double mutant in line with the faster rate of degradation (see Fig. 5). Taken together, these results suggest that N-glycosylation favors delivery to the membrane and slows down protein endocytosis and, hence, increases duration at the membrane and/or resistance to degradation. This supposition is both quantitatively and qualitatively demonstrated by western blot and confocal images, respectively (Fig. 5). Indeed, upon cyclohexymide treatment the total amount of N163Q and particularly N163/212Q decreased faster than wild type, i.e., mutants are internalized before WT; imaging confirms that at longer times WT remains associated with the plasma membrane, while glycosylation defective proteins are mainly in the cytosol (Fig. 5E). The glycosyl moiety linked to N163 has probably a major role in protein stability, as indicated by the similar behavior of the N163Q and N163/212Q mutants (Fig. 5B and D). The double mutant shows the highest impairment of both targeting and residence in membrane. The presence of spotted fluorescence especially visible in the double mutant transfected cells (see Fig. 5E) indicates that glycosylation influences also the intrinsic stability of the protein.

The results of this study may have implications in pathology, since ASCT2 is over-expressed in several human cancers [1,20]. Therefore, studying the role of glycosylation in trafficking is also important since cancer cells exhibit altered patterns of protein glycosylation. Aberrant glycosylation of cell-surface proteins has been linked to cancer-cell adhesion, invasion, and metastasis [30,44]. The glucose transporter GLUT1 experienced structural changes in the N-linked sugar chains in a human cervical carcinoma increasing the availability of glucose for transformed cells [45].

In conclusion, an essential role of N-glycosylation in trafficking and membrane stabilization of ASCT2 has been revealed in this study. Glycosylation does not correlate with functionality, since non-glycosylated ASCT2 protein, either mutated or over-expressed in yeast, is correctly inserted into artificial membranes and reaches the quaternary structure necessary to accomplish its intrinsic transport activity (see Fig. 2 and [36]). These results highlight the physiological importance of N-glycosylation as a part of the regulatory context that allows ASCT2 to function with a wide distribution of tissues and in overall amino acid homeostasis.

Transparency document

The Transparency document associated with this article can be found, in the version.

Acknowledgment

This work was supported by funds from MIUR (Ministery of Instruction, University and Research): Programma Operativo Nazionale [01_00937] — “Modelli sperimentali biotecnologici integrati per lo sviluppo e la selezione di molecole di interesse per la salute dell'uomo” to CI and by funds from the Natural Science and Engineering Research Council (NSERC, n.203397-2011-RGPIN) of Canada and from Ryerson University to IRC.

References

[1] L. Pochini, M. Scalise, M. Galluccio, C. Indiveri, Membrane transporters for the special amino acid glutamine: structure/function relationships and relevance to human health, Front. Chem. 2 (2014) 61.
[2] H.B. Schioth, S. Roshanbin, M.G. Hagglund, R. Fredriksson, Evolutionary origin of amino acid transporter families SLC32, SLC36 and SLC38 and physiological, pathological and therapeutic aspects, Mol. Asp. Med. 34 (2013) 571–585.
[3] Y. Kanai, B. Clemencon, A. Simonin, M. Leuenberger, M. Lochner, M. Weisstanner, M.A. Hediger, The SLC1 high-affinity glutamate and neutral amino acid transporter family, Mol. Asp. Med. 34 (2013) 108–120.
[4] D. Fotiadis, Y. Kanai, M. Palacin, The SLC3 and SLC7 families of amino acid transporters, Mol. Asp. Med. 34 (2013) 139–158.
[5] S. Broer, M. Palacin, The role of amino acid transporters in inherited and acquired diseases, Biochem. J. 436 (2011) 193–211.
[6] V. Torres-Zamorano, F.H. Leibach, V. Ganapathy, Sodium-dependent homo- and hetero-exchange of neutral amino acids mediated by the amino acid transporter ATB degree, Biochem. Biophys. Res. Commun. 245 (1998) 824–829.
[7] N. Utsunomiya-Tate, H. Endou, Y. Kanai, Cloning and functional characterization of a system ASC-like Na + −dependent neutral amino acid transporter, J. Biol. Chem. 271 (1996) 14883–14890.
[8] P. Pingitore, L. Pochini, M. Scalise, M. Galluccio, K. Hedfalk, C. Indiveri, Large scale production of the active human ASCT2 (SLC1A5) transporter in Pichia pastoris–functional and kinetic asymmetry revealed in proteoliposomes, Biochim. Biophys. Acta 1828 (2013) 2238–2246.
[9] F. Oppedisano, L. Pochini, M. Galluccio, C. Indiveri, The glutamine/amino acid transporter (ASCT2) reconstituted in liposomes: transport mechanism, regulation by ATP and characterization of the glutamine/glutamate antiport, Biochim. Biophys. Acta 1768 (2007) 291–298.
[10] M.M. Adeva, G. Souto, N. Blanco, C. Donapetry, Ammonium metabolism in humans, Metabolism 61 (2012) 1495–1511.
[11] B.P. Bode, Recent molecular advances in mammalian glutamine transport, J. Nutr. 131 (2001) 2475S–2485S (discussion 2486S-2477S).
[12] B.C. Fuchs, B.P. Bode, Amino acid transporters ASCT2 and LAT1 in cancer: partners in crime? Semin. Cancer Biol. 15 (2005) 254–266.
[13] K. Shimizu, K. Kaira, Y. Tomizawa, N. Sunaga, O. Kawashima, N. Oriuchi, H. Tominaga, S. Nagamori, Y. Kanai, M. Yamada, T. Oyama, I. Takeyoshi, ASC amino-acid transporter 2 (ASCT2) as a novel prognostic marker in non-small cell lung cancer, Br. J. Cancer 110 (2014) 2030–2039.
[14] V. Ganapathy, M. Thangaraju, P.D. Prasad, Nutrient transporters in cancer: relevance to Warburg hypothesis and beyond, Pharmacol. Ther. 121 (2009) 29–40.
[15] S. Broer, Targeting tumour cells at the entrance, Biochem. J. 439 (2011) e1–e2.
[16] B.C. Fuchs, R.E. Finger, M.C. Onan, B.P. Bode, ASCT2 silencing regulates mammalian target-of-rapamycin growth and survival signaling in human hepatoma cells, Am. J. Physiol. Cell Physiol. 293 (2007) C55–C63.
[17] P. Nicklin, P. Bergman, B. Zhang, E. Triantafellow, H. Wang, B. Nyfeler, H. Yang, M. Hild, C. Kung, C. Wilson, V.E. Myer, J.P. MacKeigan, J.A. Porter, Y.K. Wang, L.C. Cantley, P.M. Finan, L.O. Murphy, Bidirectional transport of amino acids regulates mTOR and autophagy, Cell 136 (2009) 521–534.
[18] M. Laplante, D.M. Sabatini, mTOR signaling in growth control and disease, Cell 149 (2012) 274–293.
[19] F. Oppedisano, M. Catto, P.A. Koutentis, O. Nicolotti, L. Pochini, M. Koyioni, A. Introcaso, S.S. Michaelidou, A. Carotti, C. Indiveri, Inactivation of the glutamine/amino acid transporter ASCT2 by 1,2,3-dithiazoles: proteoliposomes as a tool to gain insights in the molecular mechanism of action and of antitumor activity, Toxicol. Appl. Pharmacol. 265 (2012) 93–102.
[20] Q. Wang, K.A. Beaumont, N.J. Otte, J. Font, C.G. Bailey, M. van Geldermalsen, D.M. Sharp, J.C. Tiffen, R.M. Ryan, M. Jormakka, N.K. Haass, J.E. Rasko, J. Holst, Targeting glutamine transport to suppress melanoma cell growth, Int. J. Cancer 135 (2014) 1060–1071.
[21] T. Albers, W. Marsiglia, T. Thomas, A. Gameiro, C. Grewer, Defining substrate and blocker activity of alanine-serine-cysteine transporter 2 (ASCT2) Ligands with Novel Serine Analogs, Mol. Pharmacol. 81 (2012) 356–365.
[22] D. Deng, C. Xu, P. Sun, J. Wu, C. Yan, M. Hu, N. Yan, Crystal structure of the human glucose transporter GLUT1, Nature 510 (2014) 121–125.
[23] D. Yernool, O. Boudker, Y. Jin, E. Gouaux, Structure of a glutamate transporter homologue from *Pyrococcus horikoshii*, Nature 431 (2004) 811–818.
[24] F. Oppedisano, M. Galluccio, C. Indiveri, Inactivation by Hg2+ and methylmercury of the glutamine/amino acid transporter (ASCT2) reconstituted in liposomes: Prediction of the involvement of a CXXC motif by homology modelling, Biochem. Pharmacol. 80 (2010) 1266–1273.
[25] M. Scalise, L. Pochini, S. Panni, P. Pingitore, K. Hedfalk, C. Indiveri, Transport mechanism and regulatory properties of the human amino acid transporter ASCT2 (SLC1A5), Amino Acids 46 (2014) 2463–2475.
[26] N.E. Avissar, H.C. Sax, L. Toia, In human entrocytes, GLN transport and ASCT2 surface expression induced by short-term EGF are MAPK, PI3K, and Rho-dependent, Dig. Dis. Sci. 53 (2008) 2113–2125.
[27] L.B. Li, N. Chen, S. Ramamoorthy, L. Chi, X.N. Cui, L.C. Wang, M.E. Reith, The role of N-glycosylation in function and surface trafficking of the human dopamine transporter, J. Biol. Chem. 279 (2004) 21012–21020.
[28] Y. Haga, K. Ishii, T. Suzuki, N-glycosylation is critical for the stability and intracellular trafficking of glucose transporter GLUT4, J. Biol. Chem. 286 (2011) 31320–31327.
[29] H. Hayashi, Y. Yamashita, Role of N-glycosylation in cell surface expression and protection against proteolysis of the intestinal anion exchanger SLC26A3, Am. J. Physiol. Cell Physiol. 302 (2012) C781–C795.
[30] M.N. Christiansen, J. Chik, L. Lee, M. Anugraham, J.L. Abrahams, N.H. Packer, Cell surface protein glycosylation in cancer, Proteomics 14 (2014) 525–546.

[31] O. Vagin, J.A. Kraut, G. Sachs, Role of N-glycosylation in trafficking of apical membrane proteins in epithelia, Am. J. Physiol. Renal Physiol. 296 (2009) F459–F469.
[32] S.N. Ho, H.D. Hunt, R.M. Horton, J.K. Pullen, L.R. Pease, Site-directed mutagenesis by overlap extension using the polymerase chain reaction, Gene 77 (1989) 51–59.
[33] M. Galluccio, L. Pochini, V. Peta, M. Ianni, M. Scalise, C. Indiveri, Functional and molecular effects of mercury compounds on the human OCTN1 cation transporter. C50 and C136 are the targets for potent inhibition, Toxicol. Sci. 144 (2014) 105–113.
[34] M. Scalise, M. Galluccio, L. Pochini, C. Indiveri, Over-expression in Escherichia coli, purification and reconstitution in liposomes of the third member of the OCTN sub-family: the mouse carnitine transporter OCTN3, Biochem. Biophys. Res. Commun. 422 (2012) 59–63.
[35] L. Pochini, M. Scalise, M. Galluccio, C. Indiveri, Regulation by physiological cations of acetylcholine transport mediated by human OCTN1 (SLC22A4). Implications in the non-neuronal cholinergic system, Life Sci. 91 (2012) 1013–1016.
[36] K. Mochizuki, T. Kagawa, A. Numari, M.J. Harris, J. Itoh, N. Watanabe, T. Mine, I.M. Arias, Two N-linked glycans are required to maintain the transport activity of the bile salt export pump (ABCB11) in MDCK II cells, Am. J. Physiol. Gastrointest. Liver Physiol. 292 (2007) G818–G828.
[37] R. Accardi, M. Scalise, T. Gheit, I. Hussain, J. Yue, C. Carreira, A. Collino, C. Indiveri, L. Gissmann, B.S. Sylla, M. Tommasino, IkappaB kinase beta promotes cell survival by antagonizing p53 functions through DeltaNp73alpha phosphorylation and stabilization, Mol. Cell. Biol. 31 (2011) 2210–2226.
[38] T.A. Giancaspero, G. Busco, C. Panebianco, C. Carmone, A. Miccolis, G.M. Liuzzi, M. Colella, M. Barile, FAD synthesis and degradation in the nucleus create a local flavin cofactor pool, J. Biol. Chem. 288 (2013) 29069–29080.
[39] N.M. Nivillac, J. Bacani, I.R. Coe, The life cycle of human equilibrative nucleoside transporter 1: from ER export to degradation, Exp. Cell Res. 317 (2011) 1567–1579.
[40] C. Indiveri, M. Galluccio, M. Scalise, L. Pochini, Strategies of bacterial over expression of membrane transporters relevant in human health: the successful case of the three members of OCTN subfamily, Mol. Biotechnol. 54 (2013) 724–736.
[41] C.A. Filippo, O. Ardon, N. Longo, Glycosylation of the OCTN2 carnitine transporter: study of natural mutations identified in patients with primary carnitine deficiency, Biochim. Biophys. Acta 1812 (2011) 312–320.
[42] T. Asano, H. Katagiri, K. Takata, J.L. Lin, H. Ishihara, K. Inukai, K. Tsukuda, M. Kikuchi, H. Hirano, Y. Yazaki, The role of N-glycosylation of GLUT1 for glucose transport activity, J. Biol. Chem. 266 (1991) 24632–24636.
[43] T. Asano, K. Takata, H. Katagiri, H. Ishihara, K. Inukai, M. Anai, H. Hirano, Y. Yazaki, Y. Oka, The role of N-glycosylation in the targeting and stability of GLUT1 glucose transporter, FEBS Lett. 324 (1993) 258–261.
[44] I. Häuselmann, L. Borsig, Altered tumor-cell glycosylation promotes metastasis, Front. Oncol. 4 (2014) 28.
[45] T. Kitagawa, Y. Tsuruhara, M. Hayashi, T. Endo, E.J. Stanbridge, A tumor-associated glycosylation change in the glucose transporter GLUT1 controlled by tumor suppressor function in human cell hybrids, J. Cell Sci. 108 (Pt 12) (1995) 3735–3743.